



Numerical evaluation of the plastic hinges developed in headed stud shear connectors in composite beams with profiled steel sheeting

V. Vigneri*, C. Odenbreit, M. Braun

ArcelorMittal chair of steel and façade, University of Luxembourg, Luxembourg

ARTICLE INFO

Keywords:

Push-out test
Shear stud
Mechanical model
Numerical model
Shear connector with profiled sheeting

ABSTRACT

For composite beams using novel steel sheeting, the current Eurocode 4 rules sometimes overestimate the load-bearing capacity of headed stud shear connectors. This is due to the larger rib heights and the smaller rib widths in comparison with the old studies, which have been carried out to calibrate the current design equations. The RFCS Project “DISCO” investigated this phenomena and the working group under mandate M515, CEN/TC250/SC4/SC4.T3 is enhancing this equation and working on a proposal to be taken over in the new version of Eurocode 4.

The proposed new equation covers the failure behaviour of the shear connection more in detail. The test results show, that the failure consists in a combined concrete cone and stud in bending. Due to the geometry of novel steel sheeting, the load bearing capacity of the headed stud shear connector is no more limited by its shear capacity, but by its bending capacity.

A 3D non-linear finite element model is developed and validated through the support of the DISCO push-out tests. A good agreement between numerical and experimental results in terms of force-slip behaviour is achieved. Special attention of this work lies on the numerical evaluation of the number of plastic hinges n_y ; a stress-based procedure is presented and the results are compared to the equations presented for new Eurocode 4.

The numerical simulations show that the upper plastic hinge moves up as the slip increases due to the progressive crushing of the concrete in the rib. From the parametric study, it turns out that n_y is linearly proportional to the embedment depth. Compared to pre-punched hole decking, through-deck welding specimen activates less plastic hinges in the studs because of the higher stiffness provided at the base of the stud.

1. Introduction

Steel-concrete composite solutions are massively used in several sectors, especially for non-residential multi-storey buildings. Their success is mainly due to a good balance between structural performance (e.g. strength and stiffness) and economical efficiency. In view of that, more and more studies have recently focused on developing more advanced and precise technical regulations in order to increase the efficiency of steel-concrete solutions.

This contribution will focus on headed stud shear connectors used in composite beams using profiled steel sheeting with ribs transverse to the supporting beams. The steel studs are welded on the steel beam flange and are able to transfer the shear force between the concrete slab and steel beam.

The design load-bearing resistance of the aforementioned shear connectors is currently calculated through the formulation presented in EN1994-1-1 [1]. That is none other than an extension of the formula

proposed for solid slabs, reduced by a coefficient k_t calibrated in the early 1990s. Despite its simplicity, current regulations does not lead to safe and efficient results for some modern steel decking [2–5]. Therefore, several recent projects, such as the RFCS project DISCO, are aimed at developing new refined rules taking into account the mechanical behaviour of the members.

Recent push-out tests showed that “new” failure modes may occur when deep profiled steel sheeting are used: concrete cone failure in combination with a plastic bending of the headed shear studs. The new proposed equations for predicting the shear resistance of the connector presented in this paper take into account these two, parallel acting, mechanisms.

This work is mainly focused on the evaluation of the number of plastic hinges developed in the studs through numerical finite element models.

* Corresponding author.

E-mail address: valentino.vigneri@uni.lu (V. Vigneri).

<https://doi.org/10.1016/j.istruc.2019.03.017>

Received 30 November 2018; Received in revised form 18 February 2019; Accepted 27 March 2019

Available online 30 April 2019

2352-0124/ © 2019 Institution of Structural Engineers. Published by Elsevier Ltd. All rights reserved.

2. Experimental investigation

Among other experimental works, the project DISCOO (Development of Improved Shear Connector rules in COMposite beam) provided interesting results from several push-out tests [6]. A typical specimen of the tests is shown in Fig. 1.

It was observed that the specimens generally exhibit a combined “concrete cone” and “stud in bending” failure, see Figs. 2 and 3 respectively. An important outcome is that deeper steel sheeting leads to the formation of one plastic hinge at the bottom of the studs. Unlike deep sheeting, composite beams using low profiled steel sheeting are able to develop two plastic hinges due to the higher embedment of the studs provided by the concrete.

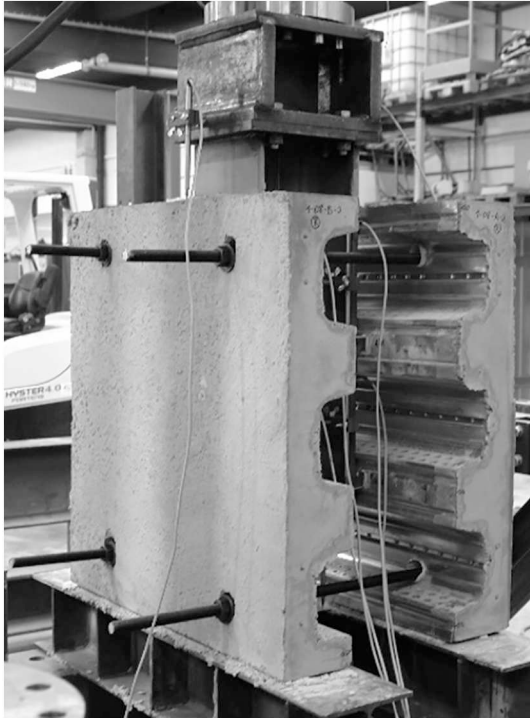


Fig. 1. Specimen of DISCOO project using 80 mm deep steel sheeting.



Fig. 2. Concrete cones observed in the push-out specimen after demounting.

3. Proposed analytical equations

3.1. General

Based on the failure modes observed, a new mechanical model has been proposed [7] and developed [8]. Unlike current rules in EN 1994-1-1 [1], this model can capture a more realistic failure behaviour of the connection. Firstly, the contribution of the concrete cone is considered as the elastic bending resistance of an equivalent cantilever, see Fig. 4. The shear force P_c carried by the concrete cone per stud is given by the Eq. (1):

$$P_c = \frac{f_{ctm} W}{n_r h_p} \quad (1)$$

where f_{ctm} is the mean tensile strength of the concrete, W indicates the section modulus of the concrete cone failure surface defined according to Eq. (2), n_r is the number of studs per rib and h_p represents the height of the rib, see Fig. 4.

$$W = [2.4h_{sc} + (n_r - 1)e_t] \frac{[\max(b_{top}, b_{bot})]^3}{6b_{top}} \quad (2)$$

The parameters indicated in Eq. (2) are based on the failure surface of the concrete cone that was firstly estimated by Lloyd and Wright [9] and then simplified.

The influence of the studs is accounted by considering an equivalent beam with one or two plastic hinges [10,11]. These two extreme cases and the relative static schemes are shown in Figs. 5 and 6, respectively. However, new investigations presented in Sections 4 and 5 were performed to obtain a more realistic and economical solution: instead of considering one or two plastic hinges, a smooth transition between these extreme cases was taken into account.

Assuming that the plastic bending moment of the cross section M_{pl} is reached, the analytical expression of the shear force P_{sc} carried by the stud can be derived:

$$P_{sc} = \frac{n_y M_{pl}}{h_s - d/2} \quad (3)$$

where n_y indicates the number of plastic hinges developed in the studs; h_s and d are defined in Figs. 5 and 6.

M_{pl} is equal to $f_u d^3/6$ where f_u indicates the specified ultimate tensile strength of the stud material, but not higher than 500 MPa in computation.

By summing the “concrete cone” (P_c) and “stud in bending” (P_{sc}) components previously described, the resultant shear resistance of the connection (per stud) P_R is given by:

$$P_R = \min \left\{ \frac{f_u A}{\sqrt{3}}, \alpha_{c2} k_u \left(\frac{f_{ctm} W}{h_p n_r} + \frac{n_y M_{pl}}{h_s - d/2} \right) \right\} \quad (4)$$

where $(f_u A/\sqrt{3})$ indicates the pure shear resistance of the stud according to Von-Mises failure criteria; A is the cross-sectional area of the stud. The coefficient of reduction α_{c2} and k_u accounts for short-term relaxation of the concrete and the position of the studs in the rib, respectively.

The principal objective of this investigation is the assessment of the load-bearing behavior of the connectors and of the studs in detail, which supports the relative design equations presented by CEN/TC250/SC4.PT3 for the revised version of Eurocode 4.

An accurate evaluation of the plastic hinges activated at low displacements only on the basis of experimental work is hardly possible; therefore, the parameter n_y is numerically evaluated through an



Fig. 3. Plastic deformation of the stud with (a) one and (b) two plastic hinges.

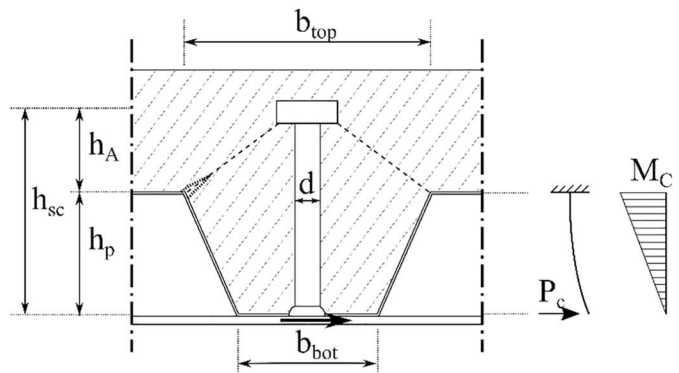


Fig. 4. Equivalent static scheme of the concrete rib of the shear connector.

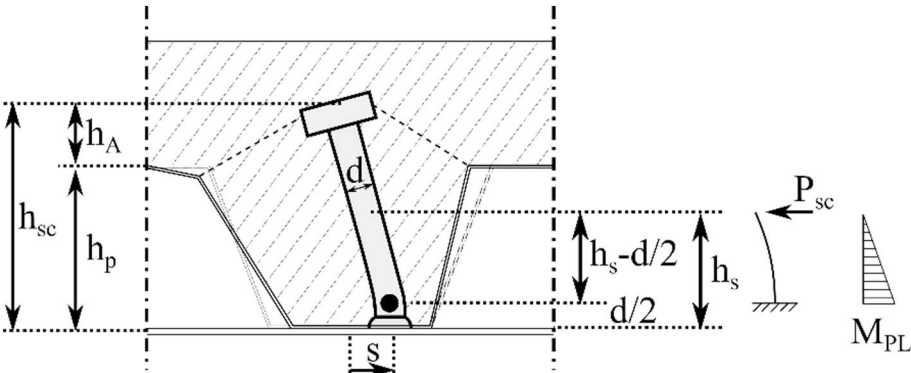


Fig. 5. Equivalent static scheme of the steel stud with one plastic hinges.

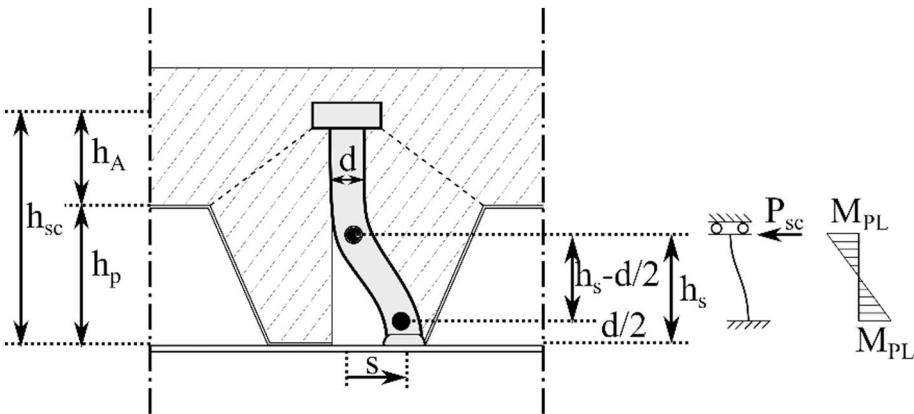


Fig. 6. Equivalent static scheme of the steel stud with two plastic hinges.

experimentally validated finite element model described in the next section.

4. Finite element model

4.1. General






The software Abaqus 6.14-5 [13] was used for numerically reproducing the push-out tests. Based on former numerical works performed on push-out tests [12], a 3D non-linear finite element model with dynamic-explicit solver is used. This helps to overcome convergence problems that generally arise at contact/interaction interfaces.

The model consisted of 5 instances: concrete slab, steel beam and studs (tied together), profiled steel decking, reinforcement mesh and steel plate. The key features of each element are listed in Table 1.

Due to the symmetry of the push-out test, only a quarter of the specimen was reproduced (Fig. 7) with proper boundary conditions. All the nodes on the bottom surface of the base steel plate were fixed in all directions. All nodes of surface 1 were fixed in X direction and the nodes of surface 2 were restrained in Y direction in order to reproduce the symmetry conditions.

Except for the base steel plate, an average mesh size of 10 mm was assessed to be suitable. General contact algorithm was adopted for modelling all the contacts. In this work, the default normal behaviour was considered for all the interactions and no tensile stress is allowed to be transferred. Penalty friction formulation was chosen for the tangential behaviour with a friction coefficient of 0.5 and 0.3 for steel-concrete and steel-steel interactions respectively. The tangential friction coefficient between the concrete slab and the base was preliminary taken as 0.8 to account for the contribution of the mortar bed. However, no significant difference in terms of resistance and mechanical behaviour was observed from additional numerical simulations when the

Table 1
Modelling parameters of the elements.

Instance	Mesh type		Failure criteria
Slab	C3D8R		CDP
Studs and beam	C3D8R		Von Mises
Rebars	T3D2		Von Mises
Sheeting	S4R		Von Mises
Plate	C3D8R		–

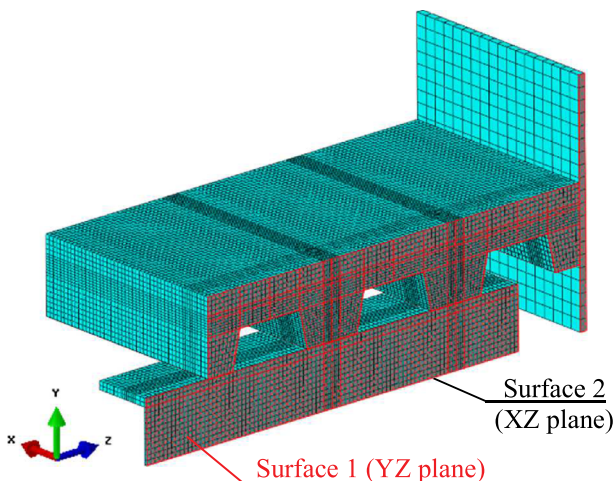


Fig. 7. Mesh of the finite element model (specimen DISCOO 3-02).

aforementioned coefficient lies in the range 0.4–0.8. For through-deck welded specimen, a tie constraint was enforced between the bottom of the stud shank and the decking hole. Conversely, no interaction/contact was considered in pre-punched hole specimen.

4.2. Load application

Due to the dynamic nature of the solver adopted, the loading rate, time period and mass scaling factor need to be carefully evaluated to minimize the dynamic-inertial effects throughout the numerical simulation. In order to ensure a quasi-static process, the kinetic energy should not exceed 5% fraction of the internal energy of the whole system.

A suitable loading rate v_0 and time period T were chosen as a function of the maximum end slip analysed, see Table 2.

Table 2
Key parameters for load application.

Max. end slip s_{end} [mm]	Time period T [s]	Loading rate [mm/s]
10	20	0.5

The loading rate was introduced gradually by using a proper smooth step function for a relatively small time $t_0 < T$. No transversal load was applied as its influence is not investigated in this work.

4.3. Material modelling

As already shown in previous numerical study on push-out test [12], the use of Concrete Damage Plasticity (CDP) model leads to satisfying results. Therefore, CDP was selected for modelling the slab in this study. The plasticity parameters adopted in the model are shown below, in Table 3.

Table 3
Plasticity parameters of CDP model.

ψ [deg]	e [-]	f_{bo}/f_{co} [-]	K_c [-]	μ [-]
38	0.1	1.16	0.67	–

Based on previous investigations [14,15], the following equations for uniaxial compressive stress-strain relation σ_c - ϵ_c were implemented:

$$\sigma_c = f_c \frac{n \left(\frac{\epsilon_c}{\epsilon_{c0}} \right)}{(n-1) + \left(\frac{\epsilon_c}{\epsilon_{c0}} \right)^n} \quad (5)$$

where f_c and ϵ_{c0} are respectively the concrete uniaxial compressive strength and the relative strain. The parameter n is given by:

$$n = 1.5 \cdot [0.058 f_c \text{ (MPa)} + 1] \quad (6)$$

The compression damage parameter d_c was calculated through Eq. (7) [16], where b_c is taken equal to 0.7 and ϵ_c^{pl} indicates the plastic compressive strain.

$$d_c = 1 - \frac{\sigma_c E_c^{-1}}{\epsilon_c^{pl} (1/b_c - 1) + \sigma_c E_c^{-1}} \quad (7)$$

Conversely, uniaxial post-crack behaviour of concrete was implemented by using an exponential stress-crack opening σ_c - w function [17] shown in Eq. (8).

Table 4
Material properties of steel elements.

Property	Beam	Decking	Stud
f_y [MPa]	424	350	470
f_u [MPa]	525	420	500
ϵ_u [-]	0.16	0.16	0.075

Table 5
Key parameters for validated push-out tests.

Reference test	3-01-3	3-02
h_p [mm]	80	80
n_r [studs/rib]	2	2
d [mm]	19	19
h_{sc} [mm]	118	123
Rebar mesh	Q188A and Q335A	Q188A
Welding	Through deck	Pre-punched holes
f_{cm} [MPa]	40.4	42.6
E_{cm} [MPa]	26,800	28,000
P_{Exp} [kN/stud]	52.78	36.99
P_{Fem} [kN/stud]	55.93	38.00
P_{Fem}/P_{Exp} [-]	1.06	1.03

$$\left\{ \begin{array}{l} \sigma_t = f_t \left[f(w) - \left(\frac{w}{w_c} \right) f(w_c) \right] \\ f(w) = [1 + (3w/w_c)^3] \exp\left(-\frac{6.93w}{w_c}\right) \\ w_c = 5.14 G_f / f_t \end{array} \right. \quad (8)$$

where w_c is the critical crack opening at which no tensile stress can be transferred. G_f is the fracture energy which is estimated according to Model Code 90 [18]. The tensile damage parameter was assumed to be linearly proportional to the tensile stress reduction after cracking:

$$d_t = \begin{cases} 0 & w = 0 \\ 1 - \frac{\sigma_t(w)}{f_t} & w > 0 \end{cases} \quad (9)$$

Measured values of Young Modulus and concrete strength of concrete were considered in the model and in the parametric studies and the Poisson ratio was fixed to 0.2.

The material of the beam and sheeting was modelled with a bilinear stress-strain law and Von Mises criteria: the main properties are listed in Table 4. A bilinear stress-strain law was also considered for the reinforcement bars where $f_y = 500$ MPa and $f_u = 550$ MPa.

The material of the shear stud behaves almost elastic-perfectly

plastic with a nearly horizontal plateau at ultimate strength f_u . However, in the numerical simulation it was conservatively assumed that the yielding of the stud material starts at $f_y = 470$ MPa with a hardening slope of 400 MPa reaching the ultimate strength $f_u = 500$ MPa at a strain of 7.5%.

4.4. Validation

In order to validate the numerical model presented, two tests from DISCO project were taken as a reference: the results were compared in terms of resistance, stiffness and then force-slip behaviour. The data and the resistance of the push-tests reproduced are listed in Table 5. As shown in Fig. 8(a) and (b), a good agreement between experimental and numerical results is achieved.

5. Numerical and analytical evaluation of the number of plastic hinges n_y

5.1. Stress-based method procedure

In order to quantify the number of plastic hinges activated in the studs, a stress-based method is presented in this paragraph. First, the normal stress distribution is obtained in the numerical model by cutting the cross-section at which the plastic hinge develops (i.e. relatively high localized normal stresses). The feature PATH is needed to obtain the normal stresses σ_N along the central nodes, see Fig. 9.

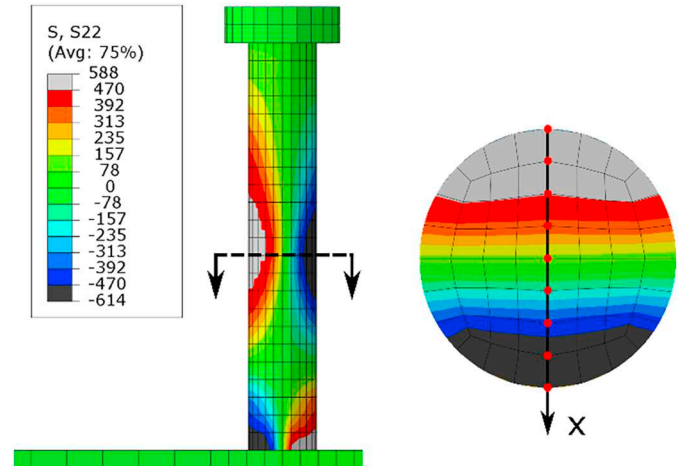


Fig. 9. Cross-section of upper plastic hinge with the relative path nodes.

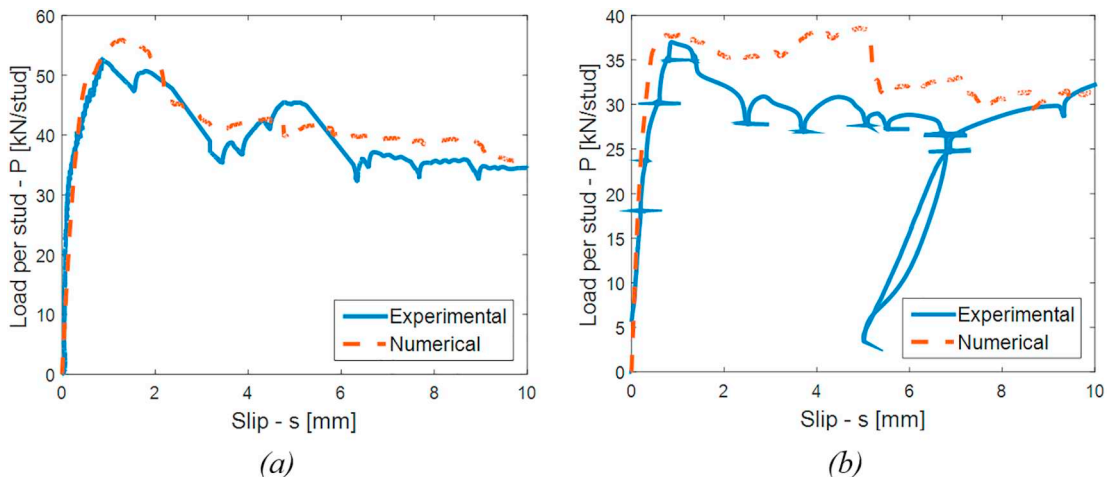


Fig. 8. Force-slip plot of DISCO test (a) 3-01-3 and (b) 3-02.

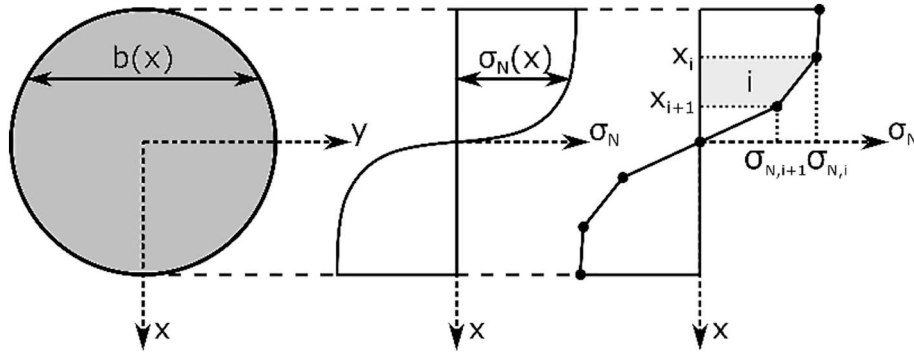


Fig. 10. Real and numerical discrete normal stress distribution along the cross-section of the stud.

Once the stress distribution $\sigma_N(x)$ is known, the bending moment can be calculated analytically by solving the following integral:

$$M_y = \int_A [\sigma_N(x) \cdot x] dA = \int_{-\frac{d}{2}}^{\frac{d}{2}} [\sigma_N(x) \cdot b(x) \cdot x] dx \quad (10)$$

where $b(x)$ is the width of the circular cross-section, which can be defined as a function of d and x :

$$b(x) = 2\sqrt{\frac{d^2}{4} - x^2} \quad (11)$$

As the normal stresses are locally calculated in the nodes, $\sigma_N(x)$ will be a piecewise linear function. Therefore, it is convenient to integrate on each interval i , see Fig. 10.

Based on the functions illustrated above, the integral in Eq. (10) can be written as follows:

$$M_y = \sum_i \int_{x_i}^{x_{i+1}} \left\{ [\sigma_{N,i} + \sigma'_{N,i}(x - x_i)] 2x \sqrt{\frac{d^2}{4} - x^2} \right\} dx \quad (12)$$

The integral expression is analytically solvable and the resulting bending moment resistance will be equal to:

$$M_y = \frac{1}{12} \sum_i \left\{ 3\sigma'_{N,i} r^4 \sin^{-1}\left(\frac{x}{r}\right) + \left[(-6\sigma'_{N,i}x - 6\sigma'_{N,i}x_i - 8\sigma_{N,i})(r^2 - x^2)^{\frac{3}{2}} \right] + 3\sigma'_{N,i}r^2x\sqrt{r^2 - x^2} \right\}_{x_i}^{x_{i+1}} \quad (13)$$

To calculate the fraction of plastic hinge activated at a certain cross-section, the bending moment M_y computed in Eq. (13) is compared to

the theoretical plastic bending capacity of the stud $M_{pl} = f_u d^3/6$, where f_u is the tensile strength of the stud material taken as 500 MPa, as shown in Table 4.

Assuming that one plastic hinge always develops at the bottom of the stud, the number of activated plastic hinges in each stud will be equal to:

$$n_y = 1 + \frac{M_y}{M_{pl}} \leq 2 \quad (14)$$

where M_y is evaluated at the height of the upper plastic hinge where the highest normal stresses are observed.

From the evaluation of the numerical results, it was found that the plastic hinge is fully activated only when the value of the bending moment M_y reaches $0.95M_{pl}$.

5.2. Parametric analysis

In addition to the two validated tests already performed, 4 numerical simulations were carried out. Only push-out tests with two studs per rib were in this study. The parameters analysed are the type of welding and the embedment depth h_A , where the latter was changed by increasing/decreasing the height of the stud h_{sc} . The slip values of 1.5, 3 and 6 mm were taken as a reference allowing one to visualize the evolution of the plastic hinge and giving a better understanding of the load-bearing mechanism of the studs.

Fig. 11(a) and (b) show the evolution of the activated plastic hinges throughout the simulation for low and high embedment depth configuration respectively.

It is also clear that the ductility of the shear connector is related to the values of the plastic hinges.

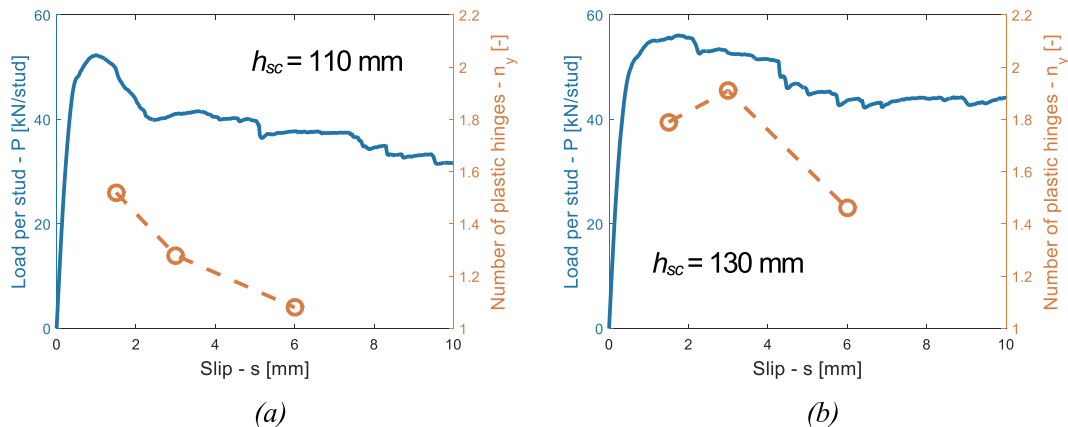


Fig. 11. Evolution of n_y in (a) low and (b) high embedment depth specimen.

Table 6
Number of plastic hinges n_y from the numerical parametric analysis.

Welding	Through deck			Pre-punched holes		
h_{sc} [mm]	110	118	130	110	123	130
$h_{A,N}$ [-]	0.79	1.00	1.32	0.79	1.13	1.32
s [mm]	1.5	1.52	1.70	1.79	1.85	1.89
	3	1.28	1.56	1.91	1.79	1.96
	6	1.08	1.33	1.46	1.41	1.81
						1.99

The results of the parametric analysis are summarized below in Table 6 as a function of the normalized embedment depth $h_{A,N}$, defined as:

$$h_{A,N} = \frac{h_A}{2d} = \frac{h_{sc} - h_p}{2d} \quad (15)$$

The results show the positive effect of the embedment depth onto the activated plastic hinges because the development of the upper plastic hinge in the stud is mainly governed by the rotational stiffness provided by the concrete part above the rib. If enough embedment depth is ensured, the concrete behaves as a “fixed” constraint and no rotation of the stud head is allowed. Conversely, the less is the embedment depth h_A , the less rotational stiffness is provided and the second hinge can develop only partially.

Compared to through-deck welding, pre-punched hole specimen exhibits higher values of number of plastic hinges at all displacements, see Table 6. This is the consequence of the extra stiffness provided at the base of the stud when the studs are through-deck welded. In this case, part of the load coming from the slab is carried not only through

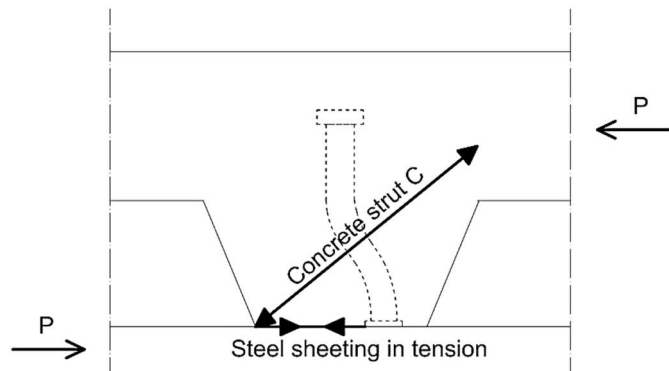


Fig. 12. Schematic of “back-anchorage” mechanism in through deck welded stud configuration.

Table 7
Vertical coordinate of the upper hinge a from the numerical parametric analysis.

Welding	Through deck			Pre-punched holes		
h_{sc} [mm]	110	118	130	110	123	130
$h_{A,N}$ [-]	0.79	1.00	1.32	0.79	1.13	1.32
s [mm]	1.5	63	64	63	58	55
	3	85	84	80	73	68
	6	90	96	95	90	78

the bending deformation of the stud, but also by tensile stresses induced in the sheeting through a “back-anchorage” mechanism shown in Fig. 12. This results in a relative reduction of the resistance component provided by the studs in bending, so the second hinge could not fully develop.

Furthermore, the normal stress σ_N contour plot of the studs over the simulation in Fig. 13 shows that the upper plastic hinges moves up until it completely “vanishes” once the head of the stud rotates due to local crushing of the underlying concrete. This so called “travelling” plastic hinge is the consequence of the progressive concrete crushing which leads to a gradual change of the stiffness centre. The vertical coordinate of the upper plastic hinge a is extrapolated at different slip and the results are listed in Table 7.

5.3. Comparison between numerical and predicted values of n_y

As already mentioned in Section 2, the parameter n_y has a key role to properly predict the load-bearing capacity of the connector, see Eq. (4). The work group CEN/TC250/SC4.PT3 proposed a simplified expression for estimating n_y defined in Eq. (16).

$$n_y = \begin{cases} 2 & n_r = 1 \\ 1 + \frac{h_{A,N} - 1}{0.26} \leq 2 & n_r = 2 \end{cases} \quad (16)$$

Specifically, for one stud per rib, the minimum embedment depth of $2d$ allowed by EN 1994-1-1 is assumed to be sufficient to ensure the formation of 2 plastic hinges. Instead, when two studs are placed in the rib, n_y is considered to be linearly proportional to the already defined normalized embedment depth $h_{A,N}$. In order to compare analytical and numerically assessed values of n_y , the reference slip of 6 mm is chosen to be the most suitable since current design rules [1] considers it as “target slip” to ensure the ductility of the connection.

Compared to the expression presented in Eq. (16), the numerical parametric study provides a lower slope of the function $n_y(h_{A,N})$, for two studs per rib, as seen in Fig. 14. Despite this difference, a smooth

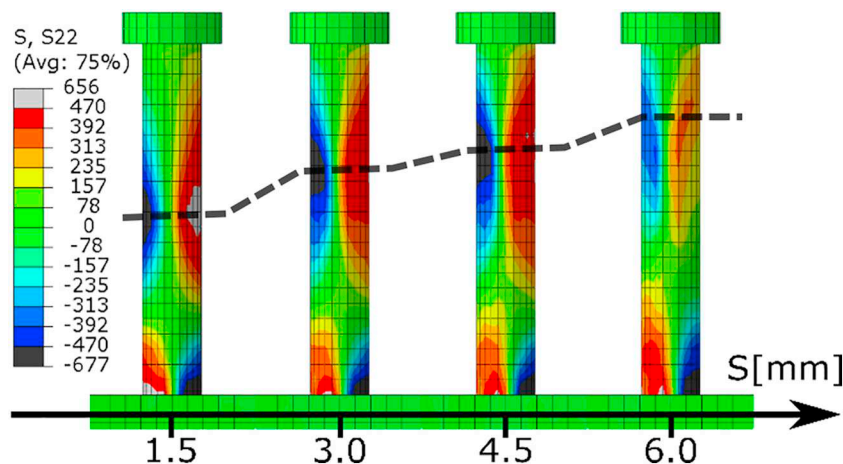


Fig. 13. Normal stress contour at an end slip of 1.5, 3, 4.5 and 6 mm (3-02 test).

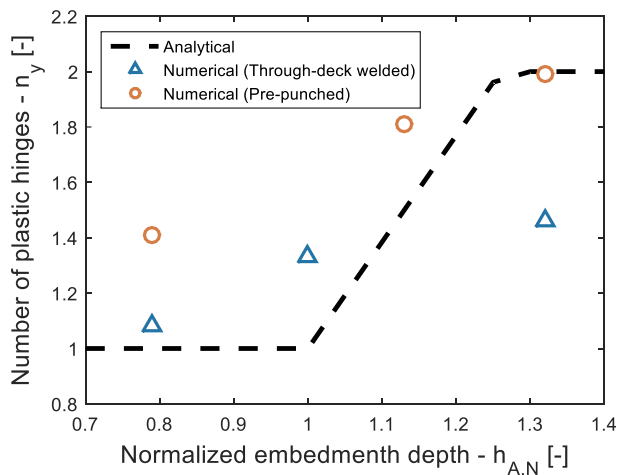


Fig. 14. Comparison between numerical and analytical results.

transition between 1 and 2 plastic hinges can be identified in both cases. However, additional geometric and mechanical parameters need to be assessed in order to estimate n_y more accurately.

6. Conclusions

The main outcomes of this contribution are:

- Based on the results observed in the push-out tests of the project DISCO [6], a mechanical model and the corresponding analytical equations for predicting the load-bearing resistance of shear connection with profiled steel sheeting are developed;
- A 3D finite element model using dynamic/explicit solver is presented and properly validated against DISCO push-out tests in terms of stiffness, capacity and ductility (up to 10 mm end-slip);
- An analytical stress-based method is proposed and used to extrapolate the number of plastic hinges in the studs from the numerical model;
- All the numerical simulations performed show that the upper plastic hinge moves up as the slip increases. This is a consequence of the progressive crushing of the concrete in the rib leading to a relocation of the centre of stiffness;
- According to the proposed stress-based procedure, the number of plastic hinges at 6 mm slip is approximately linearly proportional to the embedment depth;
- Compared to pre-punched hole decking, through-deck welding specimen exhibit lower values of activated plastic hinges due to the higher stiffness provided at the base of the stud.

7. Outlook

The influence of further design parameters such as the position of the reinforcement, the number of studs per rib and the concrete strength is still under investigation. Based on supplementary numerical studies, a refined mechanical model will be developed.

Acknowledgement

The authors gratefully acknowledge the primary funder of the research, ArcelorMittal Global R&D, Long Products Luxembourg, under the grant number UL-E-AGR-0022-10-C.

References

- [1] EN 1994-1-1, Eurocode 4: design of composite steel and concrete structures - part 1-1: general rules and rules for buildings. 2004.
- [2] Ernst S, Bridge RQ, Wheeler A. Strength of headed stud shear connection in composite beams. *Aust J Struct Eng* 2007;7(2):111–21.
- [3] Hicks SJ, Smith AL. Stud shear connectors in composite beams that support slabs with profiled steel sheeting. *Struct Eng Int* 2014;24(2):246–53.
- [4] Johnson RP, Yuan H. Existing rules and new tests for stud. *Proc Inst Civ Eng Struct Build* 1998;128(3):244–51.
- [5] Smith AL, Couchman GH. Strength and ductility of headed stud shear connectors in profiled steel sheeting. *J Constr Steel Res* 2010;66:748–54.
- [6] Odenbreit C, Kuhlmann U, Nellinger S, Eggert F. Development of improved shear connection rules in composite beams - deliverable D1.3: report on push-out test results. 2015.
- [7] Nellinger S. On the behaviour of shear stud connections in composite beams with deep decking Ph.D. Dissertation University of Luxembourg; 2015.
- [8] Odenbreit C, Vigneri V, Amadio C, Bedon C, Braun M. New mechanical model to predict the load bearing resistance of shear connectors with modern forms of profiled sheeting. *13th International Conference on Steel, Space and Composite Structures*, Perth. 2018.
- [9] Lloyd R, Wright HD. Shear connection between composite slabs and steel beams. *J Constr Steel Res* 1990;15(4):255–85.
- [10] Lungershausen. Zur Schubtragfähigkeit von Kopfbolzendübeln. Ruhr universität bochum; 1988.
- [11] Odenbreit C, Nellinger S. Mechanical model to predict the resistance of the shear connection in composite beams with deep steel decking. *Steel Constr* 2017;10(3):248–53.
- [12] Quareshi J. Finite element modelling of steel-concrete composite structures Ph.D. Dissertation University of Leeds; 2010.
- [13] Dassault Systèmes Simulia. Abaqus Analysis User's Guide v6.14. 2014.
- [14] Popovics S. A numerical approach to the complete stress-strain curve of concrete. *Cem Concr Res* 1973;3:583–99.
- [15] Thorenfeldt E, Tomaszewicz A, Jensen JJ. Mechanical properties of high strength concrete and application in design. *Symposium on utilization of high-strength concrete*, Trondheim. 1987.
- [16] Birtel V, Mark P. Parameterised finite element modelling of RC beam shear failure. *Abaqus users' conference*. 2006.
- [17] Cornelissen HAW, Hordijk DA, Reinhardt HW. Experimental determination of crack softening characteristics of normalweight and lightweight concrete. *HERON* 1986;31(2):45–56.
- [18] FIB - Fédération internationale du béton, CEB-FIP Model Code 1990: Design Code. 1993.